energies

MDPI

Article

Energy and Environmental Assessment of Cogeneration in Ceramic Tiles Industry

Maria Alessandra Ancona [1], Lisa Branchini [1,*], Saverio Ottaviano [1], Maria Chiara Bignozzi [2], Benedetta Ferrari [3], Barbara Mazzanti [3], Marcello Salvio [4], Claudia Toro [4], Fabrizio Martini [4] and Miriam Benedetti [4]

1 Department of Industrial Engineering, University of Bologna, Viale del Risorgimento 2, 40136 Bologna, Italy
2 Department of Civil, Chemical, Environmental and Materials Engineering, University of Bologna, Via Terracini 28, 40131 Bologna, Italy
3 Centro Ceramico, Joint Lab SMILE, Via Terracini 28, 40131 Bologna, Italy
4 Italian National Agency for New Technologies, Energy and Sustainable Economic Development (ENEA), Lungotevere Thaon di Revel 76, 00196 Rome, Italy
* Correspondence: lisa.branchini2@unibo.it; Tel.: +39-0512093314

Abstract: Ceramic tile manufacturing is a highly energy-intensive process. Concerns about carbon emissions and energy costs make energy management crucial for this sector, which holds a leading role in Italian industry. The paper discusses the energetic and environmental performance of cogeneration (CHP) in the ceramic industry, where prime mover exhaust heat is supplied to a spray-dryer system, contributing to the satisfaction of the thermal demand and decreasing natural gas consumption. A thermodynamic model of a dryer unit, validated against real data, has been set-up to provide a detailed representation of the thermal fluxes involved in the process. Then, the thermal integration with two types of CHP prime movers of similar electric size (4 MW) is investigated. Energetic results show that the gas turbine can contribute up to 81% of dryer thermal consumption, whilst internal combustion engine contribution is limited to 26%. A methodology was ad-hoc defined for the environmental assessment of CHP, accounting for global (CO_2) and local (CO and NO_X) emissions. Results confirm that CHP units guarantee reduction of CO_2 and NO_X compared to separate generation, with maximum values equal to 81 g/kWh$_{th}$ and 173 mg/kWh$_{th}$, respectively; CO emission is decreased only in the case of gas turbine operation, with savings equal to 185 mg/kWh$_{th}$.

Keywords: cogeneration; energy efficiency; industrial decarbonization; gas turbine; internal combustion engine; spray dryer; ceramic industry; energy analysis; environmental analysis; thermodynamic modelling

Citation: Ancona, M.A.; Branchini, L.; Ottaviano, S.; Bignozzi, M.C.; Ferrari, B.; Mazzanti, B.; Salvio, M.; Toro, C.; Martini, F.; Benedetti, M. Energy and Environmental Assessment of Cogeneration in Ceramic Tiles Industry. *Energies* **2023**, *16*, 182. https://doi.org/10.3390/en16010182

Academic Editor: Raffaello Cozzolino

Received: 1 December 2022
Revised: 19 December 2022
Accepted: 21 December 2022
Published: 24 December 2022

1. Introduction

The European Union (EU) agreed upon an ambitious target for climate neutrality by 2050, aiming to cut down about 83–87% of carbon emissions compared to 1990 levels [1]. To achieve this challenging goal, the EU will rely on mid-term and long-term strategies, with the contribution of all economic sectors called, in particular, to increase energy efficiency and boost the use of renewable energies [2,3]. According to EU Energy Statistical Country Datasheets [4], the final energy consumption of European industry (EU-27) was about 240 Mtoe in 2019, corresponding to about 25% of the total consumption, while CO_2 emissions from the manufacturing and construction sectors accounted for about 13% of the total (about 423 tonnes of CO_2 equivalent per year). At present, Europe's industrial and manufacturing sectors are facing the dual challenge of contributing to national CO_2 emission reduction targets by 2050, and safeguarding their economic competitiveness despite the significant and continuous increase of energy prices since early 2021 [5]. Significant efforts must be directed towards energy and resource intensive sectors—such as cement, ceramics, glass, food and drink, chemicals, iron and steel, oil refining, and pulp and paper—in

order to identify and implement sustainable and economically feasible solutions, helping to reduce fossil fuel consumption and the associated environmental pressure. Medium- and high-temperature industrial heat accounts for around two-thirds of industrial energy demand [6,7]. Most of this heat cannot be electrified due to cost or technical constraints; moreover, temperature requirements of many industrial applications severely limit the application potential of renewable heat technologies that are already widespread in the domestic sector. Combined heat and power (CHP) generation is, therefore, the best available solution for many key processes such as melting, drying, sterilization, baking, process heat or industrial gas management. Cogeneration can help decarbonizing hard-to-abate industrial sectors because of the efficiency enhancement over separate generation, and can provide the lowest emissions for sectors that rely on combustion fuels and that are difficult to electrify.

The ceramic industry is known to be an energy intensive sector, directly impacted by the EU Emission Trading System (ETS) scheme over the last years. In 2018 in Europe, the ceramics industry employed 338,000 people, produced about 1304 million m^2 of tiles and involved around 2000 companies, contributing to a business turnover of 30 billion euros [8]. Spain and Italy are the biggest ceramic tile producers, representing about 70% of the EU's total production. In Italy in particular, there are in total 271 companies operating in the sector, with 26,750 direct employees and a turnover of 6.2 billion euros [9]. Given the leading role of the ceramic sector in the Italian economy, promoting decisions and strategies towards the reduction of energy and greenhouse gases (GHG) is of utmost importance.

In detail, in ceramic factories that have energy-intensive processes such as drying, firing and heating, the most important criterion for competing in the global market is the energy cost, which accounts for about 33% of the production cost. About 71% of the total energy cost is related to natural gas consumption. The firing phase accounts for more than half of the total natural gas consumption, followed by spray drying [10].

Starting from the 1980s, several technologies and strategies were introduced in this sector, with the ultimate goal of reducing (or at least optimizing) the energy consumption, and thereby enhancing the economic competitiveness [11]. Most of the developments have been focused on improving the energy efficiency of kilns, such as waste heat recovery and thermal insulation, since their operation largely affects the energy consumption of the ceramic production process [12]. The concept of energy savings has evolved to the rational use of energy through the adoption of cogeneration, i.e., the exploitation of a single primary energy source for the generation of both electricity and heat. Indeed, since the ceramic tile production process requires a significant amount of electricity and heat simultaneously, throughout the whole year, the installation of CHP technologies had a significant spread starting from 1990s [11,13]. At the end of 2019, in Italy, 28 out of 153 are ceramic tile factories were equipped with CHP technologies [13,14]. Although the spread of CHP in the Italian ceramic industry has been noteworthy, most of its potential still remains unexploited. A study conducted by the Italian Energy Services Manager (GSE) has quantified an incremental techno-economic potential of thermal energy that could be generated with CHP units, in the ceramic and glass industries, equal to 4.6 GWh. [15].

The most suitable thermal user for CHP application is the spray dryer, which is the component used to remove moisture content from the slip. CHP prime mover (PM) exhaust gases are directed to the drying process, thus suppling part of the heat required [13,16,17], with consequent natural gas savings. Commonly installed PMs are gas turbine (GT) or internal combustion engine (ICE) units [13].

The energy and exergy analyses applied to CHP units installed in a ceramic factory have been presented in [18], and results show that cogeneration systems achieve 10–50% energy savings during the drying stage. Further advanced exergy analysis is detailed in [19], where the authors analyzed the performance of a CHP system under five different environment conditions. As shown in [20], the energy and exergy efficiency of a 13 MW cogeneration system installed in a ceramic factory, located in Izmir, Turkey, reach 82% and 34%, respectively. The assessment of a CHP system for the ceramic industry by

using various exergy-based economic approaches is described in [21]. Gabaldon et al. [22], in their analysis on the effects of environmental issues on the evolution of European manufacturing, show that the majority of the Spanish spray-dried powder producers have installed cogeneration units, which has made them 85% or 90% more efficient.

The primary energy savings potential of CHP, compared to separate generation (SP), is well known and measurable according to various performance criteria [23–25]. CHP production represents also a sustainable path towards the reduction of GHG emissions. However, a dedicated and recognized quantitative methodology to measure CHP production effects in terms of pollutant emissions, in comparison with SP, is missing. Indeed, CHP systems are often constrained by the same environmental regulations and air pollution emission standards applied to non-CHP energy systems. A comprehensive overview on different technical approach for CHP emissions assessment was provided in [26–28]. The environmental issues related to CHP production are analyzed in [29–36], while different methodologies for quantifying the emission of CHP and SP are discussed in [28–31], mainly linking the environmental benefit of cogeneration to the reduction of primary energy [32] or to exergy analysis effects [36]. However, the adoption of a recognized methodology to correctly indicate CHP pros in terms of pollutants reduction is still an open issue.

The work presented in this article is part of the broader context of a research project, funded by the Ministry of Environment and Energy Security, managed by ENEA in collaboration with the University of Bologna, Centro Ceramico and Confindustria Ceramica, with the aim of delineating the current status of cogeneration in the Italian ceramic tiles sector. The main goals of this study can be summarized as follows:

- providing a complete and validated thermodynamic model of a spray dryer for an accurate quantification of the energy flows involved in the process;
- assessing the contribution of cogeneration systems, based on different PM technologies, to the thermal need of the drying process;
- addressing the environmental sustainability of cogeneration compared to SP (i.e., the use of natural gas and electricity from the grid) in ceramic tiles industry.

The long-term reference value of this study is the application of energy and sustainability analyses to cogeneration systems installed in the ceramic industry. By means of a detailed thermodynamic modelling and of a methodology ad-hoc introduced for environmental performance assessment, this study quantifies the benefits (i.e., natural gas and pollutants saving) of CHP compared to separate generation. To the authors' knowledge, this study is novel in the literature for addressing the environmental impact of CHP application in the ceramic sector, taking into account both global (i.e., carbon dioxide) and local (i.e., nitrogen oxides and carbon monoxide) pollutant emissions. In the literature, the cogeneration-based ceramic industry has not been handled in terms of energetic–environmental aspects; therefore, the study outcomes may be exemplary for other ceramic enterprises around the world. The comprehensive analysis of CHP application contributes to the promotion and support of the implementation of energy efficiency strategies in the industrial sector towards environmental sustainability.

2. The Ceramic Tile Production Process

The production process of ceramic tiles begins with the storage and preparation of raw materials. This phase consists of two main operations: grinding and water content adjustment [37]. Grinding generally takes place through a wet process to obtain an aqueous suspension (named "slip"), with a typical water content of 30%. The water content adjustment uses a spray-drying technology that allows an immediate heat exchange between a hot air flow and the slip, which is transformed into a spherical granulate, called atomized, having shape and moisture content (5–6%) suitable for the subsequent pressing phase [38]. After compacting the atomized product through a continuous or discontinuous pressing phase, the unfired or "green" tile is dried to eliminate the residual water through a process of surface evaporation and interstitial diffusion. The subsequent phases can include the glazing and surface decoration of the tiles. The ceramic products are subsequently fired

in kilns until they reach the maximum temperature around 1000–1200 °C, then, they are quickly cooled. For some product types (such as "majolica" or "cottoforte"), the firing takes place according to two distinct heat treatments: the first consists of the firing of the ceramic support or "biscuit"; the second of firing the glaze and any surface decoration. After cooling, tiles can be treated by several mechanical finishing processes and then stored in deposits, after which, they are sorted and packed.

Figure 1 schematizes the ceramic production process and highlights the distribution of the main energy vectors. The electric vector is used in all phases, as it drives electric motors, compressed air, and filters, or is used to move material through conveyor belts.

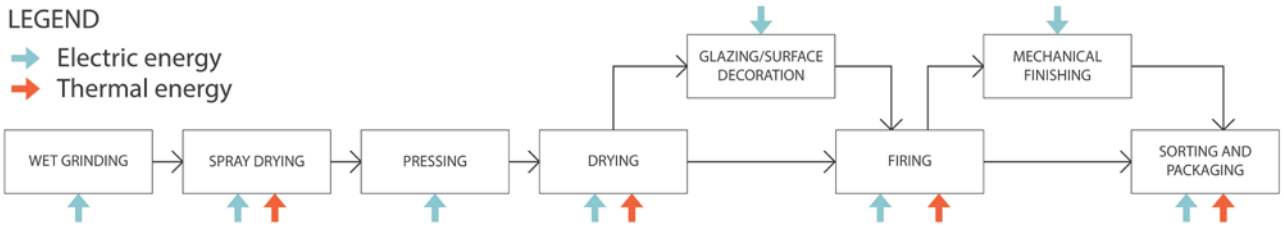

Figure 1. Distribution of energy vectors in the production process of ceramic tiles.

Approximately 70% of the total energy consumption, however, is due to the use of natural gas. Combustion of natural gas supplies the thermal energy necessary for the spray drying of the freshly formed tile bodies, as well as for the firing and packaging phases. Figure 2 shows the average percentage distribution of thermal energy consumption in the three main process phases. The highest energy consumption occurs in the firing phase, which accounts for 55% of all the thermal energy used, followed by the spray-drying phase (36%). Thermal energy used in the packaging phase generally does not exceed 1% of total consumption [39].

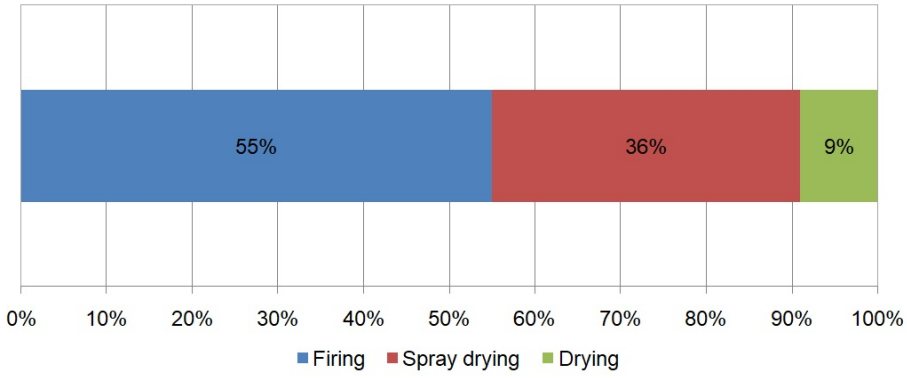

Figure 2. Breakdown of the main thermal energy consumption in ceramic tile production.

2.1. The Spray-Drying Process: Modelling and Thermodynamic Analysis

Figure 3 shows the layout of the spray dryer, the device used to remove moisture content from the slip. Slip particles are dried thanks to a hot stream (Section 5 in Figure 3) entering the top of the drying tower via a tangential peripheral aperture, at a temperature typically in the range 500–600 °C [13,38]. The characteristics of the generated vortex guarantee constant humidity and particle-size grading. Hot flue gases are generated inside a burner fed with natural gas (Section 3). The burner's inlet air flows, taken from the ambient air, are divided in two streams: combustion air (Section 1), providing the oxygen content required for the reaction with natural gas in stoichiometric condition, and pressurized air (Section 2, also known as "dilution air"), required to lower the value of the combustion gases' temperature. The presence of three fans allows for the maintenance of a constant negative pressure inside the tower. The burner-heated stream meets the slip, entering the bottom section of the tower (Section 6), finely sprayed upwards via nozzles

in the form of droplets, and guarantees moisture evaporation by convection. Thanks to the heat exchange process, an immediate evaporation and consequent hardening of the external side of the droplet take place, and simultaneously, the water vapour in the interior leaves the droplet through its rear, which collapses inwards, forming the characteristic hollow sphere appearance. Spray-dried granules, still containing typically 5–6% of water, are discharged at the bottom of the spray dryer (atomized powder stream, Section 8).

It must be noted that during spray dryer operation, a non-negligible amount of ambient air (named "false air", Section 4) inevitably enters the bottom section of the tower in the opposite direction with respect to the atomized powder flow. This flow rate is typically in the range between 8–10% of the total air flow.

The exhaust flue gases (Section 7), at temperature typically in the range 90–110 °C, is sent to the cleaning unit that allows for dust removal by means of a combination of cyclones and bag filters.

The heat required during the drying process is used, for a large part, to guarantee water evaporation; however a non-negligible amount of heat is wasted in the form of sensible heat, with exhaust gases leaving the atomizing tower. Moreover, two additional outlet energy flows are represented by the sensible heat leaving the dryer with the atomized product, and by the heat dispersed into the ambient environment through the device walls.

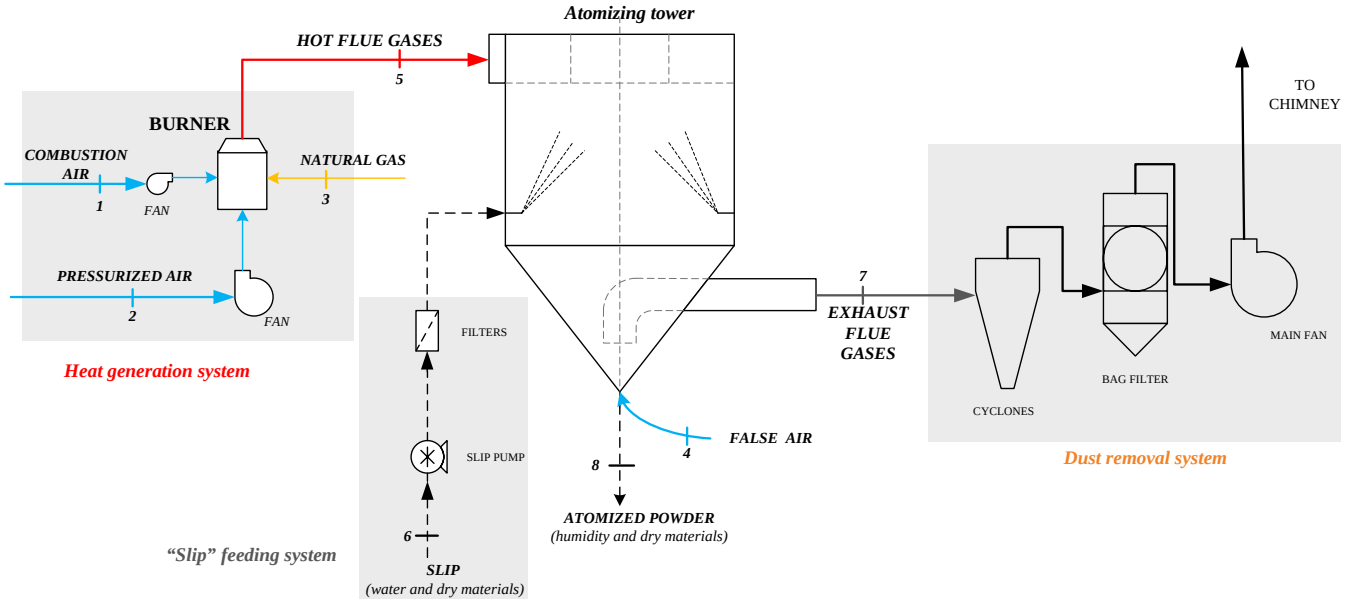

Figure 3. Schematic of the spry dryer unit.

A detailed thermodynamic analysis of the spray dryer unit has been performed in the Thermoflex environment [40] to quantify all involved energy flows and to identify the main thermodynamic conditions of gaseous streams. The software allows for the design and off-design modelling of equipment and power plants by means of a lumped parameters approach. Complex energy systems can be modelled starting from the assembly of built-in library single components and/or ad-hoc defined elements.

To this purpose, a thermodynamic model of the SACMI ATM 110 unit [41] has been built according to the schematic layout presented in Figure 3, and to the main technical data listed in Table 1. In addition, the main assumptions of the model are:

- Steady state conditions.
- Standard composition (77.30% vol. N_2, 20.70% vol. O_2, 1.00% vol. H_2O, 0.97% vol. Ar and 0.03% vol. CO_2) and ISO conditions for ambient air. Mass and volumetric flow rate of ambient air streams input, as reported in Table 2. False air stream assumed to be equal to 9% of the total air flow (combustion and pressurized) entering the tower, according to typical values [38].

- Natural gas composition with 98% vol. of CH_4 (LHV = 49,003 kJ/kg)
- Slip mass flow rate entering the tower equal to 39,780 kg/h, inlet temperature equal to 39 °C, and specific heat capacity equal to 1.21 kJ/(kg K);
- Evaporating capacity of the spray dryer unit assumed to be equal to nominal value, as in Table 1 (11 m^3/h, corresponding to 3.06 kg/s).
- Atomized powder outlet temperature and moisture content values, respectively, equal to 55 °C and 6%.
- Burner efficiency set at 98% [13].
- Heat losses through the device walls modelled according to real geometry and material, as specified in [41]. In detail, the internal walls of the tower are assumed to be stainless steel sheeting insulated with high-density mineral wool, while the external lining consists of pre-painted steel sheeting. The reference ambient temperature is assumed to be equal to 15 °C.

Table 1. Technical data of modelled SACMI ATM 110 spray dryer [41].

Nominal evaporating capacity	11 m^3/h
Nominal installed heat output	38,511 MJ/h
Tower inlet air temperature	550 °C
Slip Pump	
Maximum delivery rate	3 × 13 m^3/h
Maximum pressure	30 bar
Drying Tower	
Specific heat consumption	2.93 ÷ 3.56 MJ/kg_{H2O}
Atomized powder temperature	40 ÷ 60 °C
Atomized powder moisture content	4 ÷ 7%
Exhaust Air	
Flow rate @ 100 °C e 1 bar	105,000 m^3/h
Exhaust air temperature	60 ÷ 130 °C

Table 2. Assumed conditions of gaseous inlet streams.

		Combustion Air (Section 1, Figure 3)	**Pressurized Air (Section 2, Figure 3)**	**False Air (Section 4, Figure 3)**	**Natural Gas (Section 3, Figure 3)**
Flow rate	[kg/s]	5.65	11.77	1.57	0.209
	[m^3/s]	4.63	9.81	1.29	0.015
	[Nm^3/h]	15,800	32,920	4414	1091
Molar mass	[kg/kmol]	28.86	28.86	28.86	16.38
temperature	[°C]	15	15	15	25
Pressure	[bar]	1.013	1.013	1.013	20

2.1.1. Thermodynamic Modelling Results

Conditions of gaseous streams (hot and exhaust flue gases, respectively Section 5 and Section 7 in Figure 3) as results of modelling and simulation are listed in Table 3. Energy rate balance is summarized in Table 4 and, for easier visualization, in the Sankey diagram of Figure 4, as well.

Table 3. Main results of ATM 110 thermodynamic modelling for gaseous streams.

		Hot Flue Gases (Entering the Atomizing Tower, Section 5 in Figure 3)	Exhaust Flue Gases (Leaving the Atomizing Tower, Section 7 in Figure 3)
Flow rate	[kg/s]	17.63	22.26
	[m^3/s]	38.46	25.95
	[Nm^3/h]	49,764	67,841
Molar mass	[kg/kmol]	28.59	26.48
temperature	[°C]	550	103
enthalpy [1]	[kJ/kg]	567.1	89.8
N_2	[%vol]	75.70	60.53
O_2	[%vol]	16.17	13.21
CO_2	[%vol]	2.11	1.55
H_2O	[%vol]	5.11	23.98
Ar	[%vol]	0.92	0.73

[1] Reference conditions at 25 °C and 1 bar.

Table 4. Energy rate balance of ATM 110 spray dryer.

	Inlet Energy Rate [kW]	Outlet Energy Rate [kW]
Combustion air	−57	
Pressurized air	−119	
Natural gas	10,237	
Slip	639	
False air	−16	
Evaporated water		7673
Atomized powder		345
Thermal power dissipated through walls		462
Exhaust flue gases		1999
Losses due to burner efficiency		205
Total	***10,684***	***10,684***

The following considerations can be derived by analysing the obtained results:

- Natural gas provides an energy rate around 10,200 kW (equal to about 95% of the total inlet energy rate).
- The required natural gas flow rate is 0.209 kg/s (corresponding to 1091 Nm^3/h), resulting in a specific consumption—expressed per unit of evaporated water—equal to 3.56 MJ/kg_{H2O}, or 1.28 MJ/kg_{ATM}, with reference to atomized powder.
- Slip stream, entering the atomizing tower at 39 °C, contributes 639 kW to the inlet energy rate.
- The thermal energy rate used to preheat and evaporate the water content in the slip is equal to about 7700 kW, representing 72% of the total input supplied (see graphic representation in Figure 4).
- An amount of 19% of the input energy is lost as sensible heat, with exhaust gases leaving the atomizing tower at 103 °C; 4% of input energy is dissipated through the atomizing tower walls, while 3% leaves the tower with the atomized product.
- The hot stream requirement is just over 4.5 Nm^3 (@ 550 °C) per kg of evaporated water.

- The exhausted volumetric flow rate is equal to 67,841 Nm^3/h (humid exhaust gases), with an oxygen content equal to 13.2% vol. (see composition results in Table 3), or 17.3% vol. of oxygen, with reference to dry condition.

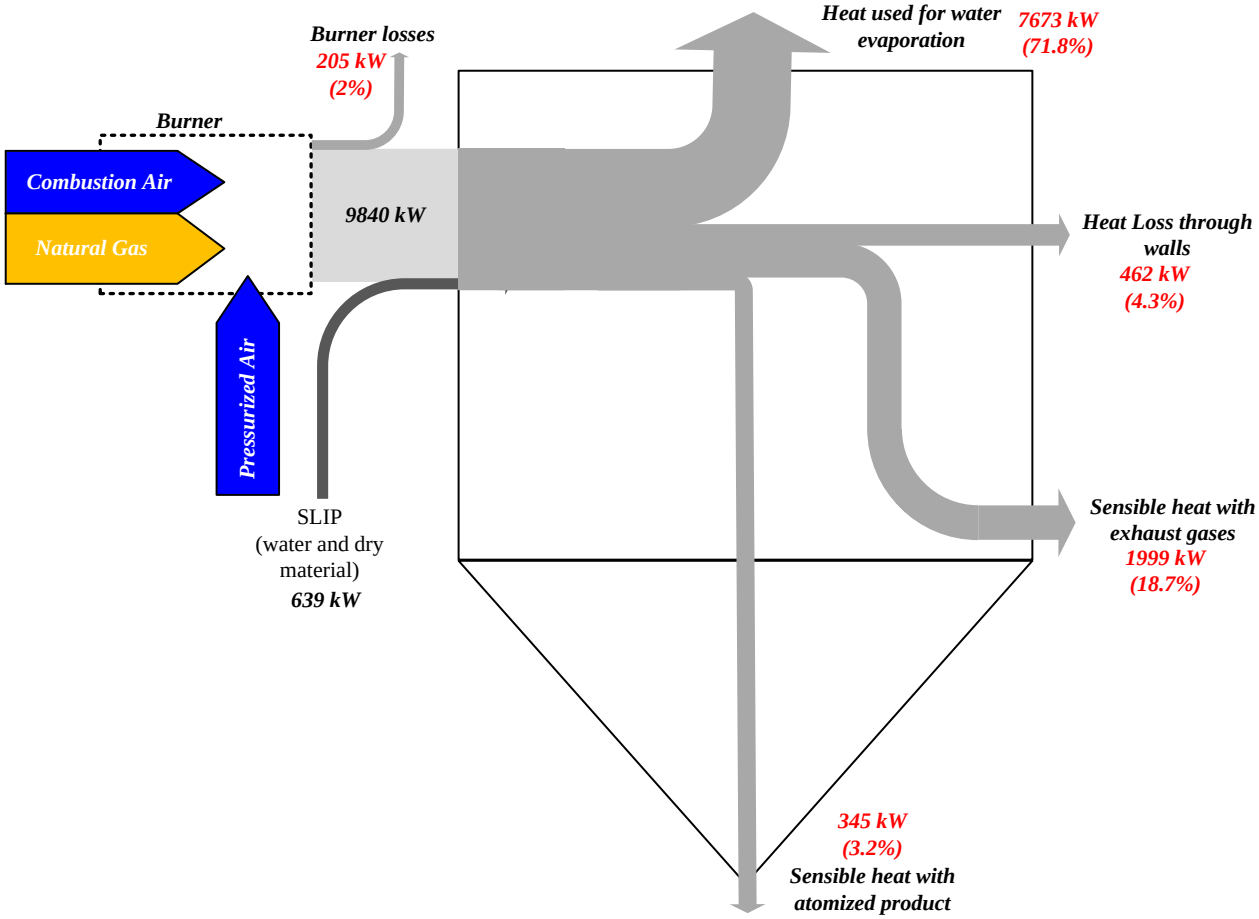

Figure 4. Sankey diagram of the ATM110 spray dryer modelled.

2.1.2. Results Validation

To validate the simulation results of Figure 4 and Table 4, a comparison with data collected from a vast campaign of direct measurements on spray dryers has been performed. Energy balances on 67 units have allowed the quantification of outlet energy flow distribution. Table 5 collects the results of the statistical analysis performed on the drier units, presented as percentage values of the input thermal energy. The analysis has allowed for the determination of mean value (x), sample standard deviation (σ), variation interval ($x \pm \sigma$) and 95% confidence interval on mean value for each of the outlet streams shown in Figure 4. No correlation with spray dryer size (i.e., evaporating capacity) has been detected for any of the investigated parameters.

Percentage values of outlet energy flows, reported in Figure 4, are in agreement with the results of Table 5, thus confirming the accuracy of the thermodynamic model. In particular, the values of the two main outlet flows resulting from the simulations (i.e., the evaporation heat and the heat discharged with exhausted) are within the 95% confidence interval of the experimental sample. The two minor contributions (heat with atomized product and heat losses through dryer walls) present larger deviation, still remaining within the total variation interval.

It can be noticed that the dispersion of the data related to the heat losses through the walls is the highest amongst the evaluated variables, as confirmed by the high ratio between the standard deviation and the average value (around 0.68). Indeed, this contribution of

loss is affected by the type of material used for the walls' thermal insulation, and by the ambient temperature, which could be different from case to case.

Table 5. Results of the energy balance analyses performed, on direct measurements, on 67 spray drier units.

Streams	Heat for Water Evaporation	Heat with Exhausted	Heat with Atomized Product	Heat Loss through Walls
mean value, x [%]	**72.6**	**17.9**	**2.4**	**2.8**
sample standard deviation, σ [p.p.]	4.4	4.4	0.9	1.9
variation interval, x ± σ [%]	[68.2; 76.9]	[13.5; 22.3]	[1.5; 3.3]	[0.9; 4.7]
95% confidence interval [%]	[71.6; 73.7]	[16.9; 18.9]	[2.2; 2.6]	[2.35; 3.25]

3. CHP Systems Supplying the Drying Process

The CHP system provides electrical energy to satisfy, fully or partially, the electricity demand of the production process, while rejected heat is directed towards the spray dryer unit as a thermal user. Indeed, in the production chain of ceramic tiles, spray drying is the preferred process for the exploitation of CHP exhausted heat [13]: PM exhaust gases are used, replacing ambient air and reducing the natural gas required to achieve the desired operating temperature (550 °C see Table 1). Gas turbine and internal combustion engine are the two CHP technologies currently used in the ceramic tiles industry [13]. Figure 5 shows the simplified layouts of CHP prime movers (GT in Figure 5a, and ICE in Figure 5b) thermally integrated with a spray-dryer. In case of ICEs, a low-grade heat source is also available: engine cooling water is typically used to preheat the pressurized air stream (as shown in Figure 5b); a heat exchanger is placed upstream from the fan component to increase the temperature of the pressurized air, typically up to 80–90 °C.

Regardless of the type of CHP prime mover, exhaust gases are heated up to the optimal operating temperature thanks to a post-combustion in the after-burner unit (see Figure 5). The main difference between the arrangements lies in the amount of fresh air used in the drying process. Indeed, exploiting exhausts coming from a GT unit allows for the use of a small fraction of fresh air coming from the ambient environment, which is pressurized by means of a fan ("pressurized air" Figure 5a). If the mass flow of the exhausts is sufficient to support the drying process, the fresh air flow could be unnecessary. Conversely, the direct use of ICE exhaust gases requires a more significant amount of fresh air. Thus, as visible in Figure 5b), both streams ("combustion air" and "pressurized air") are considered in this configuration. The pressurized air stream is mixed with ICE exhaust and post combustion takes place, introducing the combustion air inside the after-burner.

Differences between PM set-ups are mostly related to: (i) different exhaust gases mass flow rate values for GT and ICE for a given electrical size, and (ii) different concentration of oxygen in the exhaust. In detail, for the same electric size, ICEs are characterized by higher electrical efficiency compared to GTs, thus leading to a lower amount of thermal power discharged (both in terms of mass flow rate and temperature). In addition, the oxygen concentration in exhaust gases is different: GT exhaust is typically characterized by an oxygen concentration within 18–19% vol. dry, while ICE oxygen concentration is lower; in between 14–15% vol. dry. The lower oxygen concentration requires, in the case of ICEs use, an increase of the amount of fresh air needed.

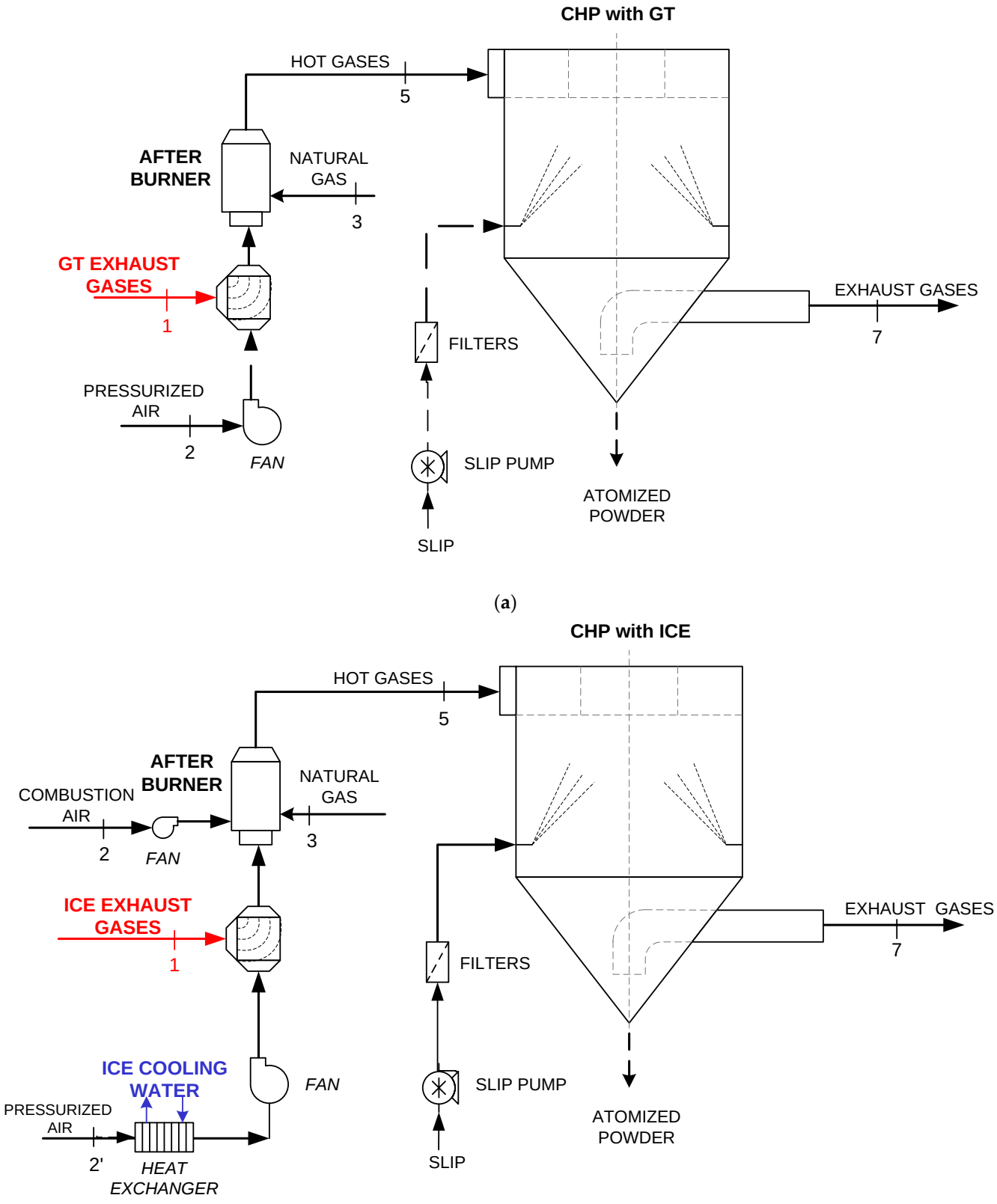

Figure 5. Schematic layout of the thermal integration between CHP and spray dryer, (**a**) with GT, (**b**) with ICE.

3.1. Energetic Analysis of CHP Systems

A preliminary investigation of installed CHP units in the Italian ceramic industries, detailed in [13], outlined the average characteristics of PMs installed. The results highlighted that the designed electric size is between 3.4 MW and 4.9 MW, with an average value equal to 4 MW. The most diffused layout is a single pair configuration, where a single CHP unit is installed to feed a single spray dryer [13].

To perform an energetic assessment of cogeneration systems used for supplying the ceramic tile production process, the numerical models of two CHP prime movers (a gas turbine and an internal combustion engine), thermally integrated with the SACMI ATM 110 unit, have been developed in the Thermoflex environment [40]. Among commercial units available in the software's library, the choice has been made according to the most popular installed models, and with reference to an electric size close to the average value (4 MW) formerly identified. The main nameplate characteristics of the selected models are listed in Table 6.

Table 6. Main characteristics for selected CHP PM units [40].

	GT Unit	**ICE Unit**
Model	General Electric GE LM500	Jenbacher JMS 624 GS
Electric power output	3880 kW	4490 kW
Electric efficiency	29.9%	47.0%
Exhaust mass flow rate	16.14 kg/s	6.53 kg/s
	45,711 Nm^3/h	18,673 Nm^3/h
Exhaust temperature	513 °C	333 °C

Different electric and thermal characteristics distinguish the selected units of similar size. The electric performance of the ICE, reaching 47% in terms of efficiency, is appreciably higher compared to the GT value (close to 30%). Accordingly, the amount of heat discharged is higher in the case of GT compared to ICE: GT exhaust gases' temperature value is up to 500 °C, with a mass flow rate of 16 kg/s. The heat that could be recovered, assuming cool down exhaust until 100 °C, reaches 7.4 MW for the GT unit, against 1.7 MW for ICE. To improve ICE thermal efficiency, engine cooling water should be exploited as well, which could recover about 1 MW of additional thermal power (i.e., 11% of fuel input power). The comparison between CHP units is, therefore, aimed at highlighting the different contribution to the drying process' thermal demand.

3.1.1. Energetic Results: Spray Dryer with GT

With reference to the schematic layout shown in Figure 5a, the thermal integration of the GT unit with the spray dryer has been modelled and investigated. The gas turbine is supposed to work at design point. The intake and exhaust ducts' pressure losses have been accounted for in the simulations. The main results of the inlet and outlet gaseous streams are listed in Table 7.

Table 7. Main results of gaseous streams for ATM 110 thermally integrated with GT unit.

		Pressurized Air (Section 2, Figure 5a)	**GT exh. Gases (Section 5, Figure 5a)**	**Natural Gas (Section 3, Figure 5a)**	**Hot Gases (Section 5, Figure 5a)**	**Exhaust Gases (Section 7, Figure 5a)**
Flow rate	[kg/s]	1.624	15.98	0.029	17.63	22.26
	[m^3/s]	1.331	33.98	0.0022	38.60	26.02
	[Nm^3/h]	4,653	45,260	150	49,943	68,019
Molar mass	[kg/kmol]	28.86	28.49	16.38	28.49	26.41
temperature	[°C]	15	527	25	550	103

Table 7. *Cont.*

		Pressurized Air (Section 2, Figure 5a)	GT exh. Gases (Section 5, Figure 5a)	Natural Gas (Section 3, Figure 5a)	Hot Gases (Section 5, Figure 5a)	Exhaust Gases (Section 7, Figure 5a)
enthalpy	[kJ/kg]	−10.13	546	49,003	573	90.30
N_2	[% vol.]	77.30	75.1	-	75.09	60.12
O_2	[% vol.]	20.70	14.43	-	14.40	11.91
CO_2	[% vol.]	0.03	2.90	-	2.91	2.14
H_2O	[% vol.]	1.00	6.67	-	6.70	25.1
Ar	[% vol.]	0.97	0.90	-	0.90	0.72

The following observations can be derived:

- Compared to stand-alone operation of the spray dryer, the exploitation of GT exhaust gases eliminates the need for fresh combustion air and drastically reduces the pressurized air flow rate (see Table 2 for comparison).
- The thermal input to the drying process provided with GT exhaust (Section 5, Figure 5a) is around 8700 kW, representing 81% of the total process need.
- As a consequence, natural gas consumption for drying (Section 3, Figure 5a) is reduced down to 0.029 kg/s (150 Nm^3/h). A fuel savings equal to 86% is achieved compared to the stand-alone non-CHP configuration. The LHV fuel input is equal to 1400 kW, corresponding to about 13% of the total heat input.
- The exhaust gases' (Section 7, Figure 5a) volumetric flow rate, equal to 68,019 Nm^3/h, keeps close to its original value (67,841 Nm^3/h, see Table 3), while the oxygen content is reduced down to 11.9% vol. (or 15.9% vol. with reference to dry condition).
- The water content in the exhaust stream leaving the atomizing tower was found to be equal to 25% vol., remaining close to the original value (23.98% vol.).
- No substantial differences were observed, compared to the non-CHP configuration, in terms of outlet energy flows: water heating and evaporation still required 72% of the total heat input, sensible heat with exhausted and atomized powder accounted, respectively, for 19% and 3% of the input energy, and heat dissipated through walls reached 4.6% of the energy input value.

3.1.2. Energetic Results: Spray Dryer with ICE

With reference to the layout presented in Figure 5b, the thermal integration between the ICE unit and the spray dryer was modelled and analysed. The results are shown in Table 8. As anticipated, the low-grade heat from the engine cooling water is recovered to increase the temperature level of the pressurized air stream. The intake and exhaust ducts' pressure losses are also accounted for in the modelling, and the internal combustion engine is assumed to be working at design point.

Table 8. Main results of gaseous streams for ATM 110 thermally integrated with ICE unit.

		Combustion and Pressurized Air (Section 2 and 2′, Figure 5b)	ICE exh. Gases (Section 1, Figure 5b)	Natural Gas (Section 3, Figure 5b)	Hot Gases (Section 5, Figure 5b)	Exhaust Gases (Section 7, Figure 5b)
Flow rate	[kg/s]	10.96	6.53	0.151	17.63	22.26
	[m^3/s]	8.98	10.62	0.011	38.69	26.06
	[Nm^3/h]	30,639	18,673	779	50,062	68,138
Molar mass	[kg/kmol]	28.86	28.2	16.38	28.42	26.36
temperature	[°C]	15	333	25	550	103

Table 8. *Cont.*

		Combustion and Pressurized Air (Section 2 and 2′, Figure 5b)	ICE exh. Gases (Section 1, Figure 5b)	Natural Gas (Section 3, Figure 5b)	Hot Gases (Section 5, Figure 5b)	Exhaust Gases (Section 7, Figure 5b)
enthalpy	[kJ/kg]	64.83	337	49,003	576	90.69
N_2	[% vol.]	77.29	73.34	-	74.67	59.84
O_2	[% vol.]	20.74	9.38	-	13.22	11.05
CO_2	[% vol.]	0.03	5.19	-	3.45	2.54
H_2O	[% vol.]	1.01	11.21	-	7.76	25.85
Ar	[% vol.]	0.93	0.88	-	0.90	0.72

The following observations can be made:

- Compared to the use of the GT unit, the volumetric flow rate of combustion and pressurized air (Section 2 and 2′, Figure 5b) remains noteworthy: the total air flow rate required is equal to 30,639 Nm^3/h.
- Thanks to exploitation of ICE low grade heat, the temperature of pressurized air is increased up to 86 °C.
- The heat recovered with ICE exhausted (Section 1, Figure 5b) is lower compared to the GT value. This reduction is linked to a lower value of exhaust gas flow rate (18,673 Nm^3/h of ICE against 45,260 Nm^3/h of GT) and temperature (333 °C of ICE versus 527 °C of GT).
- The contribution of exhaust gases to the total thermal demand achieves 21% in the case of ICE, which is still significant, but appreciably lower compared to the GT value. Low-grade heat, which increases the enthalpy level of pressurized air, allows for the covering of an additional 5% of the heat input.
- The natural gas consumption (Section 3, Figure 5b) in this configuration remains important, equal to 0.151 kg/s (or 779 Nm^3/h, see Table 8). A reduction equal to 28%, compared to spray dryer stand-alone operation, is reached.
- The exhaust stream (Section 7, in Figure 5b) results of Table 8 show a flow rate value equal to 68,138 Nm^3/h, which is almost unchanged compared to results of Table 3. Stream composition shows a reduction in the oxygen content instead (11% vol. in Table 8 compared to the 13.21% vol. value of Table 3).
- As for the GT case, as well as with ICE the distribution of energy output flows, with reference to the total thermal input, it remains unchanged compared to non-CHP configuration.

3.1.3. Results Validation

For validation purposes, the energetic results of the two investigated CHP configurations have been compared with the data of Italian ceramic companies where cogeneration units are in operation. The processing of energy audit data, as detailed in [13], allowed for the collection of the results (circular black marks) presented in Figure 6. The figure plots' percentage fraction of total heat consumption of the spray dryer (E_{th}) covered with CHP discharged heat ($E_{th,\,CHP}$), according to the definition of Λ in Equation (1).

$$\Lambda = \frac{E_{th,\,CHP}}{E_{th}} \quad (1)$$

The comparison with the modelled CHP configurations (green square marks in Figure 6) confirms that the thermal contribution is strictly dependent on the type of CHP prime mover installed, and that the obtained values are in line with real CHP operational data.

In conclusion, measuring the performance of prime movers with similar size, the gas turbine unit provides a higher contribution, compared to the combustion engine, regarding the thermal demand of the spray drying process. Nevertheless, combustion engines are often the preferred choice of the ceramic industry due to their higher electric performance [13].

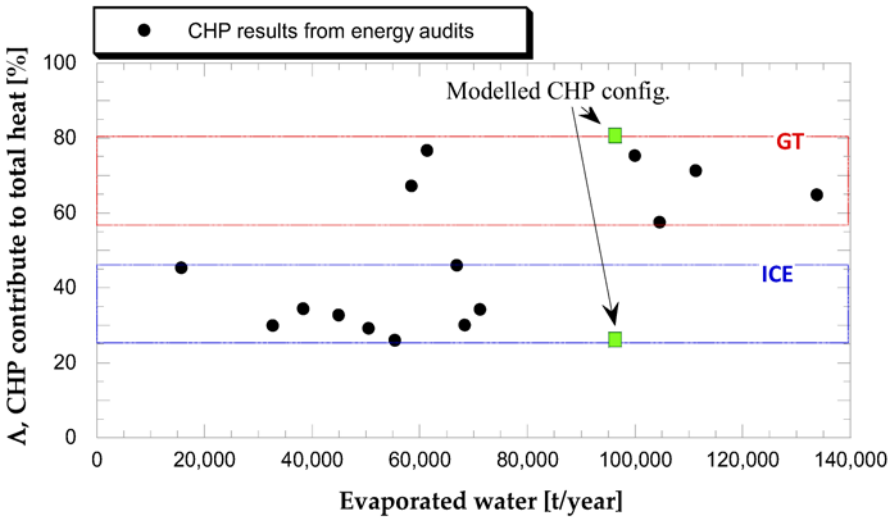

Figure 6. Percentage contribution of CHP thermal energy to total heat required by drying process as function of annual evaporated water. CHP results from energy audits [13].

4. Environmental Analysis of CHP

The pursued aim of a CHP system should be to contextually minimize the primary energy consumption and the environmental pressure. Therefore, an environmental assessment has to be included for an in-depth comprehensive analysis of combined generation. An overview of different technical methods for CHP emission assessment was provided in [27,28]; however, as stated in the introduction, the adoption of a universally recognized approach to correctly indicate CHP pros in terms of pollutant reduction is still an open issue.

4.1. Methodology Adopted

In this study, a methodology is proposed to measure the CHP environmental performance in terms of CO_2, CO and NO_X emissions. The proposed output-based approach compares the CHP scenario with a non-CHP scenario, given an equal total amount of thermal energy input to the user (i.e., the dryer). Indeed, the importance of expressing the amount of pollutant emissions of energy systems per unit of energy is relevant in the framework of a cost/benefit assessment. The specific emission, δ_i, for each pollutant species, is defined according to Equation (2):

$$\delta_i \left[\frac{\text{mg}}{\text{kWh}_{th}} \right] = \frac{\Delta_i}{E_{th}} \tag{2}$$

where Δ_i is the mass of the *i-th* species generated and E_{th} is the thermal energy input to the drying process.

As highlighted in Figure 7, a rigorous evaluation of the CHP scenario for the case studies must also include, in the assumed control volume, the operation of the after-burner unit. Indeed, as noted above, the thermal energy generated by the CHP system ($E_{th,CHP}$) represents a meaningful contribution to the dryer process; however, as confirmed by the results of Figure 6, a certain amount of natural gas is still required for exhaust gases post-combustion.

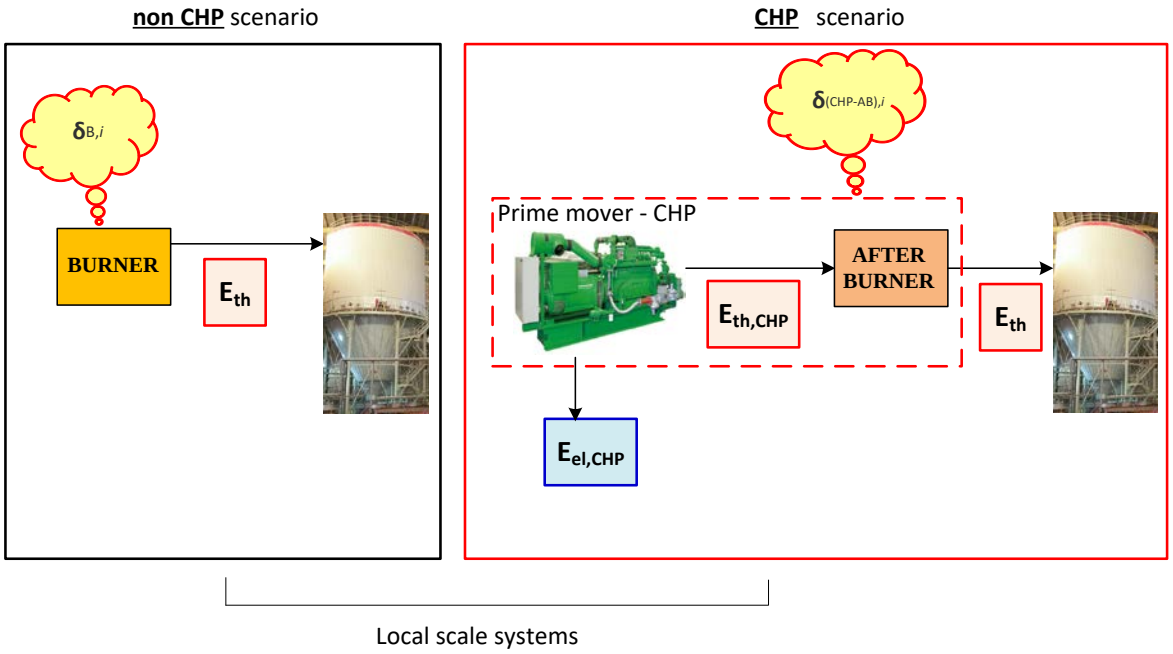

Figure 7. Emission assessment scenarios.

According to Figure 7, $\delta_{B,i}$ represents the specific emission of the *i-th* species, generated in the non-CHP scenario due to burner operation; $\delta_{(CHP-AB),i}$ refers to specific emission generated in the CHP scenario and accounting for emissions of the CHP unit and of the after-burner.

The assessment of CHP emissions should take into account that the CHP prime movers provide a double useful output, namely, electricity and thermal energy. According to the analysis performed in [13], in the majority of Italian ceramic factories, the design and the load regulation strategy of the CHP units are targeted to meet the electrical request of the manufacturing process, thus self-consuming all of the electricity produced.

Thus, in the case of the CHP scenario, a correction term should be introduced in Equation (2):

$$\delta_{new,i}\left[\frac{\text{mg}}{\text{kWh}_{th}}\right] = \delta_{(CHP-AB),i} - \delta_{avoid,i}\cdot\Lambda \tag{3}$$

where $\delta_{new,i}$ is the corrected specific emission of the system in CHP operation, $\delta_{avoid,i}$ is the avoided emission term, in comparison with the non-CHP operation. Λ is the non-dimensional parameter expressing the contribution of CHP thermal energy to the total process need (see definition in Equation (1)). Typical values of Λ are plotted in Figure 6.

In detail, the correction term is expressed as:

$$\delta_{avoid,\,i}\left[\frac{\text{mg}}{\text{kWh}_{th,CHP}}\right] = \delta_{\,el,i}\cdot\frac{\eta_{el,CHP}}{\eta_{th,CHP}} \tag{4}$$

where $\eta_{el,CHP}$ and $\eta_{th,CHP}$ represent the electric and thermal efficiency of the PM working in CHP mode, while $\delta_{\,el,i}\left[\frac{\text{mg}}{\text{kWh}_{el,CHP}}\right]$ is the output-based emission factor of a reference scenario generating only electricity. In the manufacturing processes, as an alternative to the use of a cogenerator, electricity is typically provided by the national grid. The national grid output-based emission factors are listed in Table 9 [42]. It can be observed that by increasing the environmental performance of the reference scenario considered for electricity generation (i.e., increasing the penetration of renewables would reduce $\delta_{\,el,i}$ values), the CHP benefit is reduced (i.e., $\delta_{avoid,i}$ decreases).

Table 9. National grid emission factor, $\delta_{el,i}$, for pollutant species, reference to 2018 values [42].

Pollutant Specie	Value
NO_X [mg/kWh$_{el}$]	218.4
CO [mg/kWh$_{el}$]	93.4
CO_2 [g/kWh$_{el}$]	444.4

A parametric investigation has been performed to assess the influence of the CHP PM conversion efficiencies on the avoided emission term for each pollutant species considered in the study. Figure 8 shows the results of the sensitivity analysis, where typical values of the parameter $\frac{\eta_{el,CHP}}{\eta_{th,CHP}}$ are highlighted, based on typical values of GTs and ICEs MW-size commercial units.

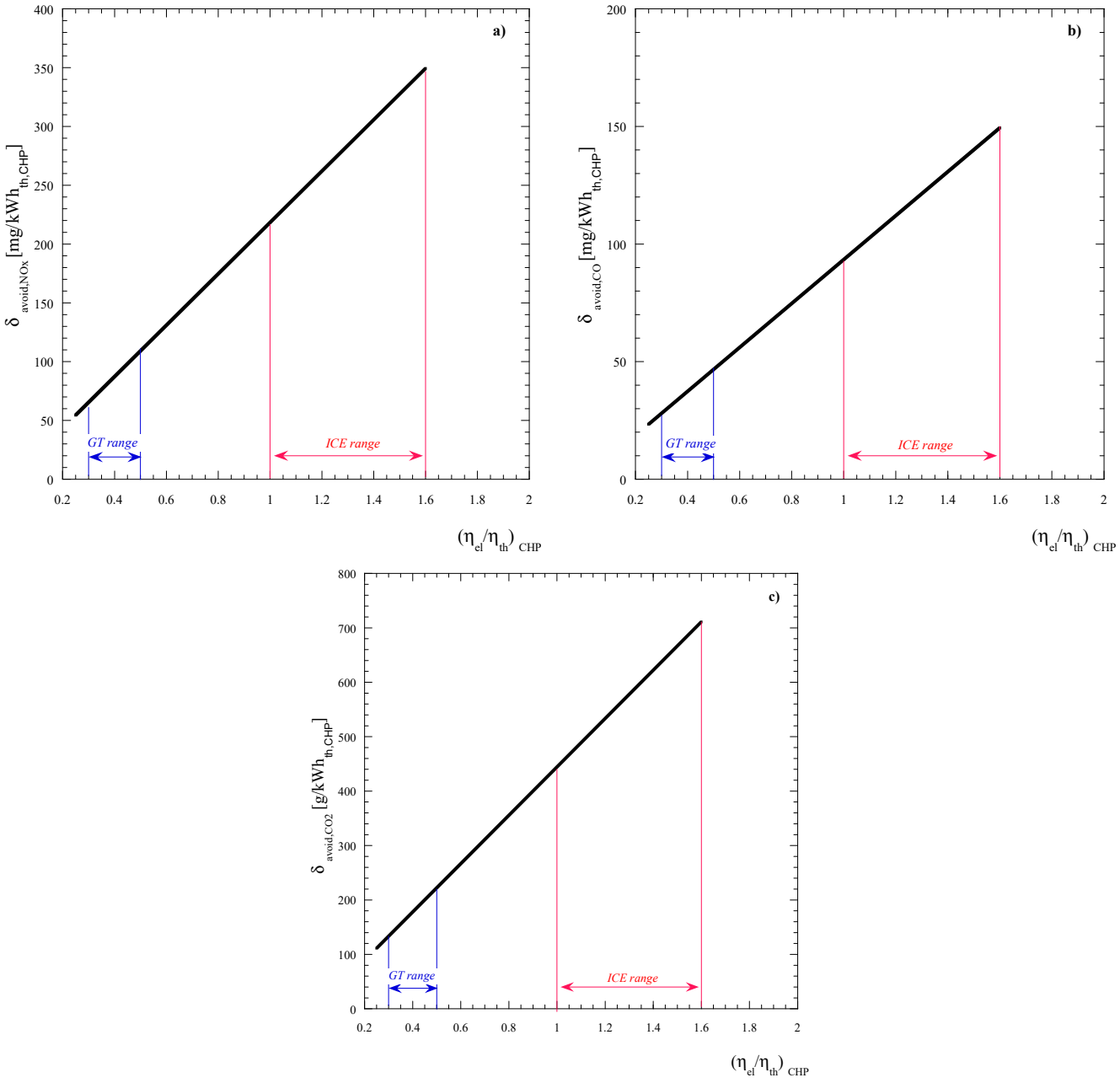

Figure 8. Avoided specific emission factor as function of CHP efficiencies ratio; (**a**) NO_X, (**b**) CO, (**c**) CO_2.

Regardless of the type of emission analyzed, results show that ICE prime movers, being characterized by higher electric efficiency, can achieve higher values of $\delta_{avoid,\ i}$ compared to GTs. Specific emissions avoided can range from 50 to 350 mg/kWh$_{th}$ in case of NO_X (see Figure 8a), from 25 to 150 mg/kWh$_{th}$ for CO (see Figure 8b), and from 100 to 700 g/kWh$_{th}$ for CO_2 (see Figure 8c).

Specific emission savings can be finally calculated as:

$$\delta_{saved,i}[\text{mg/kWh}_{th}] = \delta_{B,i} - \delta_{new,i} \quad (5)$$

4.2. Case Studies Results

The environmental performance (mass flow rate and concentration values) of the two CHP scenarios (with reference to PMs selected model of Table 6) are presented in Table 10, together with the performance achieved in the non-CHP scenario (i.e., burner operated with natural gas). The obtained values have been found to be in line with concentration values guaranteed by the ATM system manufacturer [43].

Based on the approach and the methodology described above, the specific output-based emission factors obtained are shown in Table 11. Comparing scenarios, both CHP configurations lead to significant savings of NO_X (173 mg/kWh$_{th}$ in the case of ICE and 147 mg/kWh$_{th}$ for GT). The percentage reduction realized for nitrogen oxides ranges from 55% to 64%, compared to the non-CHP scenario.

A reduction of CO is observed only with the adoption of the GT unit (185 mg/kWh$_{th}$, corresponding to 83%), while the use of an ICE as a CHP prime mover leads to an increase of CO-specific emissions compared to the non-CHP configuration. Finally, a lower impact in terms of CO_2 emissions is achieved for both CHP configurations. The achievable CO_2 savings, equal to 29% and 41%, are higher in the case of GT use compared to ICE (81 g/kWh$_{th}$ and 57 g/kWh$_{th}$, respectively).

Table 10. Pollutant emission results for non-CHP and CHP scenarios.

	Non-CHP Scenario	***CHP Scenario with ICE***	***CHP Scenario with GT***
	Mass flow rate		
NO_X [kg/h]	2.75	1.92	2.04
CO [kg/h]	2.29	7.63	0.74
CO_2 [kg/h]	2028	3361	2826
	Concentration *(dry exhaust gases 5% vol. O_2)*		
NO_X [mg/Nm^3]	236	99	126
CO [mg/Nm^3]	197	395	46
CO_2 [g/Nm^3]	174	174	174

Table 11. Environmental results, expressed as specific emissions, for the case study scenarios.

	NON-CHP Scenario	***CHP Scenario with ICE***			***CHP Scenario with GT***		
	$\delta_{B,i}$	$\delta_{(CHP+AB),i}$	$\delta_{new,i}$	$\delta_{saved,i}$	$\delta_{(CHP+AB),i}$	$\delta_{new,i}$	$\delta_{saved,i}$
NO_X [mg/kWh$_{th}$]	269	188	96	173	201	122	147
CO [mg/kWh$_{th}$]	224	749	709	−485	73	39	185
CO_2 [g/kWh$_{th}$]	198	330	141	57	279	117	81

5. Conclusions

In this study, energy and environmental sustainability analyses are applied to cogeneration systems supporting a ceramic tile manufacturing process. The cogeneration systems

consist of a gas turbine and an internal combustion engine of similar electric size (4 MW). CHP-generated electrical energy is used to satisfy the electricity demand of the production process, while prime mover rejected heat is used to feed the spray-drying process.

First, a detailed thermodynamic model of the spray dryer unit, validated against real data, is presented, allowing for the quantification of all the energy flows involved in the process, as well as for the identification of the main thermodynamic conditions of the inlet and outlet gaseous streams. Then, the thermal integration of the dryer unit with cogeneration systems is investigated, providing the contribution of each CHP prime mover to the drying process' thermal need.

Finally, a sustainability assessment of the CHP units was performed, based on a methodology ad-hoc introduced, accounting for the double useful output (electricity and heat) provided and considering both global (CO_2) and local (CO and NO_X) pollutant emissions.

The main conclusions drawn from the present study are given below:

- The thermal energy used to preheat and evaporate the moisture content in the slip accounts for 72% of the total heat input to the spray dryer unit. Sensible heat with exhaust air and atomized powder account, respectively, for 19% and 3% of the input energy. The heat losses through the dryer walls reach 4% of the input energy.
- The exploitation of exhaust gases from the gas turbine cogeneration system provides 81% of the dryer thermal need, corresponding to 941 Nm^3/h of natural gas savings.
- The internal combustion engine, having higher electric efficiency, makes available a lower amount of heat that can be recovered. It provides natural gas savings equal to 312 Nm^3/h, thereby suppling up to 26% of the input heat to the spray dryer.
- The CHP scenarios, compared to separate generation, lead to significant NO_X savings: 173 mg/kWh_{th} in the case of ICE and 147 mg/kWh_{th} for GT. A reduction of CO emissions is observed only with the adoption of the GT unit (185 mg/kWh_{th}). CO_2 savings are observed for both CHP arrangements: higher values are obtained in the case of GT use compared to ICE (81 g/kWh_{th} and 57 g/kWh_{th}, respectively).

In the framework of a cost/benefit assessment, future work will analyze the economic performance of the CHP systems.

Author Contributions: Conceptualization, L.B.; Formal analysis, L.B., B.F. and B.M.; Methodology, L.B.; Resources, L.B. and B.M.; data curation & validation B.F., B.M., F.M. and M.S.; Supervision, M.C.B. and F.M.; Writing—original draft, L.B., B.F., M.B., F.M., M.S., M.B. and C.T.; Writing—review & editing, M.A.A. and S.O.; project administration M.C.B., F.M., M.S., M.B. and C.T. All authors have read and agreed to the published version of the manuscript.

Funding: The research activity has been funded by the Electrical System Research (PTR 2019–2021), implemented under Programme Agreements between the Italian Ministry for Environment and Energy Security and ENEA, CNR, and RSE S.p.A.

Data Availability Statement: The data presented in this study are available on request from the corresponding author. The data are not publicly available due to third party restrictions.

Conflicts of Interest: The authors declare no conflict of interest.

References

1. European Commission. *A Clean Planet for All. A European Strategic Long-Term Vision for a Prosperous, Modern, Competitive and Climate Neutral Economy*; European Commission: Brussels, Belgium, 2018.
2. Ros-Dosdá, T.; Fullana-i-Palmer, P.; Mezquita, A.; Masoni, P.; Monfort, E. How can the European ceramic tile industry meet the EU's low-carbon targets? A life cycle perspective. *J. Clean. Prod.* **2018**, *199*, 554–564. [CrossRef]
3. Directorate-General for Climate Action (European Commission). *Going Climate-Neutral by 2050. A Strategic Long-Term Vision for a Prosperous, Modern, Competitive and Climate-Neutral EU Economy*; European Commission: Brussels, Belgium, 2019.
4. European Commission, EU Energy Statistical Country Datasheets. Available online: https://energy.ec.europa.eu/data-and-analysis/eu-energy-statistical-pocketbook-and-country-datasheets_en#country-datasheets (accessed on 5 October 2022).
5. European Environment Agency. *National Emissions Reported to the UNFCCC and to the EU Greenhouse Gas Monitoring Mechanism*; European Environment Agency: Copenhagen, Denmark, 2019.

6. International Energy Agency, Clean and Efficient Heat for Industry, IEA, 2018, Paris. Available online: https://www.iea.org/commentaries/clean-and-efficient-heat-for-industry (accessed on 5 October 2022).
7. Agathokleous, R.; Bianchi, G.; Panayiotou, G.; Aresti, L.; Argyrou, M.C.; Georgiou, G.S.; Tassoub, S.A.; Jouhara, H.; Kalogirou, S.A.; Florides, G.A.; et al. Waste Heat Recovery in the EU industry and proposed new technologies. *Energy Proc.* **2019**, *161*, 489–496. [CrossRef]
8. Monteiro, H.; Cruz, P.L.; Moura, B. Integrated environmental and economic life cycle assessment of improvement strategies for a ceramic industry. *J. Clean. Prod.* **2022**, *345*, 131173. [CrossRef]
9. Available online: http://www.confindustriaceramica.it/site/en/home/news/articolo9281.html (accessed on 10 July 2022).
10. Caglayan, H.; Sohret, Y.; Caliskan, H. Thermo-ecologic evaluation of a spray dryer for ceramic industry. *Energy Proc.* **2018**, *144*, 164–169. [CrossRef]
11. Agrafiotis, C.; Tsoutsos, T. Energy saving technologies in the European ceramic sector: A systematic review. *Appl. Therm. Eng.* **2001**, *2121*, 1231–1249. [CrossRef]
12. Ruivo, L.; Russo, M.; Lourenço, R.; Pio, D. Energy management in the Portuguese ceramic industry: Analysis of real-world factories. *Energy* **2021**, *237*, 121628. [CrossRef]
13. Branchini, L.; Bignozzi, M.C.; Ferrari, B.; Mazzanti, B.; Ottaviano, S.; Salvio, M.; Toro, C.; Martini, F.; Canetti, A. Cogeneration Supporting the Energy Transition in the Italian Ceramic Tile Industry. *Sustainability* **2021**, *13*, 4006. [CrossRef]
14. Confindustria Ceramica. *Indagini Statistiche Sull'industria Italiana*; Confindustria Ceramica: Sassuolo, Italy, 2019. Available online: http://www.confindustriaceramica.it/site/en/home/bookstore/studi-di-settore/indagine-statistica-sullindustria-italiana----piastrelle-di-ceramica.html (accessed on 21 October 2022).
15. Available online: https://fire-italia.org/wp-content/uploads/2021/06/2021-06-Benedetti.pdf (accessed on 20 July 2022).
16. Golman, B.; Julklang, W. Simulation of exhaust gas heat recovery from a spray dryer. *Appl. Therm. Eng.* **2014**, *73*, 899–913. [CrossRef]
17. Golman, B.; Julklang, W. Analysis of heat recovery from a spray dryer by recirculation of exhaust air. *Energy Convers. Manag.* **2014**, *88*, 641–649. [CrossRef]
18. Caglayan, H.; Caliskan, H. Energy, exergy and sustainability assessments of a cogeneration system for ceramic industry. *Appl. Therm. Eng.* **2018**, *136*, 504–515. [CrossRef]
19. Caglayan, H.; Caliskan, H. Advanced exergy analyses and optimization of a cogeneration system for ceramic industry by considering endogenous, exogenous, avoidable and unavoidable exergies under different environmental conditions. *Renew. Sustain. Energy Rev.* **2021**, *140*, 110730. [CrossRef]
20. Yoru, Y.; Karakoc, T.H.; Hepbasli, A. Dynamic energy and exergy analyses of an industrial cogeneration system. *Int. J. Energy Res.* **2009**, *34*, 345–356. [CrossRef]
21. Caglayan, H.; Caliskan, H. Assessment of a cogeneration system for ceramic industry by using various exergy based economic approaches. *Renew. Sustain. Energy Rev.* **2022**, *167*, 112728. [CrossRef]
22. Gabaldón-Estevan, D.; Criado, E.; Monfort, E. The green factor in European manufacturing: A case study of the Spanish ceramic tile industry. *J. Clean. Prod.* **2014**, *70*, 242–250. [CrossRef]
23. Directive 2004/08/EC of the European Parliament and of the Council. *Official Journal of the European Union*; European Union: Maastricht, Netherlands, 21 February 2004; pp. 50–60.
24. *US Federal Regulation, 18 C.F.R., PART 292, e-CFR 2013*; Office of the Federal Register: Washington, DC, USA, 2013.
25. Martens, A. The energetic feasibility of CHP compared to separate production of heat and power. *Appl. Therm. Eng.* **1998**, *18*, 935–946. [CrossRef]
26. Gullı', F. Small distributed generation versus centralised supply: A social cost–benefit analysis in the residential and service sectors. *Energy Policy* **2006**, *34*, 804–832. [CrossRef]
27. Bianchi, M.; De Pascale, A. Emission Calculation Methodologies for CHP Plants. *Energy Procedia* **2012**, *14*, 1323–1330. [CrossRef]
28. Bianchi, M.; Branchini, L.; De Pascale, A.; Peretto, A. Application of environmental performance assessment of CHP systems with local and global approaches. *Appl. Energy* **2014**, *130*, 774–782. [CrossRef]
29. Canova, A.; Chicco, G.; Genon, G.; Mancarella, P. Emission characterization and evaluation of natural gas-fueled cogeneration microturbines and internal combustion engines. *Energy Convers. Manag.* **2008**, *49*, 2900–2909. [CrossRef]
30. European Commission, IPPC. *Reference Document on Best Available Techniques on LCP, May 2005*; European Commission: Brussels, Belgium, 2005.
31. Hill, R.; Mortimer, N. Environmental implications. *Appl. Energy* **1996**, *53*, 89–117. [CrossRef]
32. Meunier, F. Co- and tri-generation contribution to climate change control. *Appl. Therm. Eng.* **2002**, *22*, 703–718. [CrossRef]
33. Mancarella, P.; Chicco, G. Global and local emission impact assessment of distributed cogeneration systems with partial-load models. *Appl. Energy* **2009**, *86*, 2096–2106. [CrossRef]
34. Fumo, N.; Mago, P.J.; Chamra, L.M. Emission operational strategy for combined cooling, heating, and power systems. *Appl. Energy* **2009**, *86*, 2344–2350. [CrossRef]
35. Mancarella, P.; Chicco, G. Assessment of the greenhouse gas emissions from cogeneration and trigeneration systems. Part II: Analysis techniques and application cases. *Energy* **2008**, *33*, 418–430. [CrossRef]
36. Rosen, M.A. Allocating carbon dioxide emissions from cogeneration systems: Descriptions of selected output-based methods. *J. Clean. Prod.* **2008**, *16*, 171–177. [CrossRef]

37. Maroncelli, M.; Timellini, G.; Evangelisti, R. *I Consumi Energetici Nella Produzione Delle Piastrelle Ceramiche*; Centro Ceramico: Ocotlán, Mexico, 1985.
38. SACMI. *Applied Ceramic Technology*; Editrice la Mandragora: Imola, Italy, 2002; Volume 2.
39. Mezquita, A.; Boix, J.; Monfort, E.; Mallol, G. Energy saving in ceramic tile kilns: Cooling gas heat recovery. *Appl. Therm. Eng.* **2014**, *65*, 102–110. [CrossRef]
40. Thermoflow. *Thermoflex v. 29*; Thermoflow: Jacksonville, FL, USA, 2022.
41. Available online: https://sacmi.com/SacmiCorporate/media/ceramics/Catalogues/ATM-Sacmi-(EN-IT-ES).pdf (accessed on 15 September 2022).
42. Istituto Superiore per la Protezione e la Ricerca Ambientale—ISPRA. *Fattori di Emissione Atmosferica di Gas ad Effetto Serra Nel Settore Elettrico Nazionale e Nei Principali Paesi Europei*; Rapporti 317-2020; Istituto Superiore per la Protezione e la Ricerca Ambientale—ISPRA: Roma, Italy, 2020; ISBN 978-88-448-0992-8.
43. Costa, D.; SACMI, Imola, Italy. Personal communication, 2022.